Enhanced inflammatory cell profiles in schistosomiasis-induced pulmonary vascular remodeling

Zahara Ali[1], Djuro Kosanovic[2], Ewa Kolosionek[1], Ralph T. Schermuly[2], Brian B. Graham[3], Alistair Mathie[1] and Ghazwan Butrous[1]

[1]University of Kent, Medway School of Pharmacy, Chatham, Kent, UK; [2]Universities of Giessen and Marburg Lung Center (UGMLC), Member of the German Center for Lung Research (DZL), Giessen, Germany; [3]Department of Medicine, University of Colorado, Denver, CO, USA

Abstract

Schistosomiasis (bilharzia) is a neglected parasitic disease caused by trematode flatworms of the genus *Schistosoma* which affects over 240 million people worldwide. It is characterized by the formation of inflammatory granulomas around deposited parasite eggs. Recent studies have revealed that immune and inflammatory responses play a crucial role in pathogenesis of schistosomiasis. The aim of this paper is to systematically evaluate the number and distribution of inflammatory cells in *S. mansoni*-infected mice at different doses and time points. Immunohistochemistry was performed on lung and liver tissue sections from *Schistosoma*-infected mice and uninfected healthy controls. Positively stained cells in whole-lung/liver tissue sections, surrounding the eggs, and in the different compartments of the tissues, were counted. We found a significant increase in the number of mast cells (toluidine blue^{+}), CD3^{+} cells, CD14^{+} cells, CD68^{+} cells, and CD15^{+} cells in *Schistosoma*-infected tissues compared with untreated healthy controls ($P \leq 0.05$ for all). Our findings revealed altered and enhanced immune cell infiltration in schistosomiasis. We suggest that these cells may contribute to the pathophysiology of *Schistosoma* resulting in pulmonary vascular remodeling.

Introduction

Schistosomiasis, also known as bilharzias, is a parasitic disease caused by trematodes which affects more than 240 million people worldwide. Humans become infected with different species of *Schistosoma* following exposure to water contaminated by skin penetrating cercariae.[1–4] The immunological reaction of schistosomiasis (anti-egg response) is probably the source of the pathogenesis and pathophysiology that are orchestrated by granulomatous inflammation.[1–4] The response, in the mouse model, primarily consists of proinflammatory cytokines and chemokines (type-1 T-cell response) which later switches to type-2 T-cell response. The T-cells, B-cells, antibodies, mast cells, macrophages, and dendritic cells as well as inflammatory cytokines and chemokines are typical characteristics of this granulomatous mesh.[1–4] Although these reactions will help in

the destruction of eggs, it can induce other reactions such as pulmonary vascular remodeling.

Taking advantage of the previous studies from our lab,[5] we noticed that 92% of the lungs harvested from infected mice contained evidence of granulomatous changes, secondary to egg deposition.[5] Furthermore, in 46% of lungs we witnessed vessel remodeling in close proximity to the granuloma and no remodeling was observed in the absence of granulomas.[5] Subsequent studies by the Schistosomiasis-Pulmonary Vascular Research Institute (PVRI) taskforce have summarized that inflammatory cells, via their release

Corresponding author:
Ghazwan Butrous, Medway School of Pharmacy, University of Kent, Chatham, Kent ME4 4AG, UK.
Email: g.butrous@kent.ac.uk

of multiple cytokines and chemokines, can contribute to the remodeling process, and interleukin-1 (IL-1), interleukin-4 (IL-4), interleukin-5 (IL-5), interleukin-6 (IL-6), interleukin-10 (IL-10), interleukin-13 (IL-13), transforming growth factor-β (TGF-β), and interferon-γ (IFN-γ) have been correlated with the development of pulmonary hypertension (PH).[6–8] Although several mechanisms of cellular immune-mediated vascular injury are conceivable,[6–10] the pathogenic significance of infiltrating cells in Sistosome granuloma is still poorly understood, which is the subject of this short communication.

Thus, knowledge about the mechanisms of regulation of these inflammatory mediators may help in elucidating the physiological consequences and to build the model for pulmonary vascular remodeling. A first step toward this goal is to map the most active cellular components in the granuloma that may contribute to secretion of inflammatory mediators. In this report, we evaluated the number and cross-sectional distribution of inflammatory cells viz. mast cell, CD3^{+}, CD14^{+}, CD15^{+}, and CD68^{+} in 8, 12, and 14 weeks' post-infection with *Schistosoma mansoni* (*S. mansoni*), respectively.

Materials and methods

Schistosomiasis infection

We have two groups with different methods of infection and duration between infection and sacrifice. The female mice (aged 5–6 weeks) of group I and group II were bred and housed under specific pathogen-free conditions. The protocols and surgical procedures were approved by the local ethical committees of the Natural History Museum, London, UK; the University of Kent, UK; and the University of Colorado, Denver, USA. The details of groups I and II are discussed below.

Group I (prepared in the Natural History Museum, London, UK and the University of Kent, UK): A Belo Horizonte strain of *S. mansoni* was used in all experiments. Female standard outbred BKW adult mice were infected with a suspension containing 100 cercariae (maintained at the Natural History Museum, London, UK). Briefly, mice were paddled in the warm snail water for approximately 30 min. At the end of the infection period, the mice were transferred back into their cages. The cercariae matured into worms and laid eggs at the 5th week of infection. Most pathology in schistosome-infected animals was maximal by the 8th week of infection. The animals were sacrificed after 8 (n = 10) and 12 (n = 10) weeks post infection, including the control non-infected mice (n = 5). Group I pointed out the qualitative and quantitative histopathological aspects of granulomas following natural infection via cercariae only. We used a unique BKW strain and these animals developed schistosoma in a more natural way as this occurs in humans. The morphometric analysis of the granulomas and pulmonary vessels are explained in Kolosionek et al.[5]

Group II (prepared in the University of Colorado, Denver, USA), *S. mansoni* (infected n = 4), control (non-infected mice, n = 2): The mice were given a dose of 35 cercariae/mouse (NMRI strain) by restraining the mice with their tail in a vial of water containing the cercariae for 30 min. The mice were then euthanized after 99 days (~14 weeks) post-infection with *S. mansoni*. The lung and liver paraffin blocks were sent from the School of Medicine, University of Colorado, Denver to the University of Kent. For increasing the strength of the study the non-infected controls of the two groups, i.e. groups I and II, were clubbed (n = 7) and used as one control group for comparison throughout the study. For further details on animal treatment, tissue preparation and protocols for groups I and II, please see the references.[5,7]

Tissue preparation

Lung and liver: The right lung lobe and liver were washed with saline followed by 4% formaldehyde infusion into the trachea. Next, lungs were removed and placed in 4% formaldehyde for 24 h. After this time, they were placed in 1 × PBS for 24 h, followed by dehydration and paraffin embedding (Tissue processor ASP200; Leica, Heidelberg, Germany). The specimens were stained with hematoxylin & eosin (H&E) according to standard protocols to assess the integrity of tissues. The left lung was washed with saline and frozen at −80°C for future investigations.

Mast cell histochemical staining

Toluidine blue staining was used to detect mast cells, as previously described.[9] After deparaffinization, the sections were soaked for 2–3 min in a solution of 1% toluidine blue, pH 2.2 (Sigma, Munich, Germany). The staining solution was then drained off and sections were dehydrated in 96–100% ethanol for 20–30 s, dipped in xylene, and coverslipped carefully.

Immunohistochemistry and quantification

Formalin-fixed paraffin-embedded blocks of lung tissue infected with *S. mansoni* and non-infected healthy lungs were mounted on positively charged glass slides (R. Langenbrinck, Teningen, Germany). From each tissue block, sections of 3-μm thickness were obtained and immunohistochemistry was performed. The lung tissue sections were deparaffinized in xylol and re-hydrated in a graded ethanol series. Antigen retrieval was performed by pressure cooking in Rodent Decloaker (Biocare Medical) for ~20 min following blocking with bovine serum albumin (10%) for 1 h. Primary antibodies against the following proteins were used: (1) CD3^{+} cells: CD3 (1:200; Biocare Medical, Pike Lane Concord, CA, USA); (2) CD14^{+} cells: CD14 (1:20; Zytomed, Berlin, Germany); (3) CD15^{+} cells: CD15 (1:10; Santa Cruz, Dallas, TX, USA); (4) CD68^{+} cells: CD68 (1:50;

Novus Biologicals, Southpark Way, Littleton, CO, USA); and incubation with each antibody was carried out overnight at 4°C. Development of the signals was achieved by alkaline phosphatase method and Warp red chromogen kit (Biocare), followed by the counterstain with H&E. The slides were dehydrated in absolute ethanol and xylol and cover-slipped using mounting medium. For positive controls, mouse spleen was used. Specificity of antibodies was demonstrated in negative control sections of the lung tissue (primary antibody absent). Every fifth section was selected, labeled, and stained. Images were captured by Leica DFC290 HD digital camera (Leica) and transferred to a computer containing software for image analysis. The sections were examined under a Leica DM 2500 microscope using Leica QWin imaging software (Leica).

Cell counting

The positively stained cells were counted in whole tissue sections by light microscopy (Leica Instruments, Nussloch, Germany) using ImageJ software (National Institutes of Health, Bethesda, MD, USA). Inflammatory cell counts were quantified as total number of cells per mm^2 tissue. All experiments were performed in a coded format, with the investigators lacking knowledge of the specific experimental group identifiers before final data reporting. Microscopic evaluation was carried out in a timely manner without any reduction in the color intensity. The coefficient of variation for repeat cell counts for the same observer for each antibody was <5%. We also confirmed that inter-observer coefficients of variation were <10% for all antibodies used in the study.

Statistical analysis

Data are presented as the mean ± standard error of the mean (SEM). Graphical and statistical analyses were performed with GraphPadPrism5 (GraphPad, San Diego, CA, USA). Statistical comparisons between two groups were performed using paired and unpaired Student's t-tests with Welch correction, where appropriate, with a probability value of $P < 0.05$ considered to be statistically significant.

Results

As mentioned previously, pulmonary vascular remodeling correlates with the local presence of granulomas, with remodeled pulmonary vessels, were seen in 46% of the lungs in close proximity to the granuloma.[5] These findings encouraged us to trace the actual source of inflammation; therefore, we mapped the cells of immune system in the same animal model used in Kolosionek et al.[5] Table 1 represents the analysis of immune cells in Schistosoma-infected and non-infected healthy controls.

Mast cells profile

There was a progressive increase in the number of mast cells, in particular in the area adjacent to the granulomas in the lung and liver (Fig. 1a–g). The increase was seen as early as eight weeks (group I) (0.054 ± 0.02 versus 0.0 ± 0.0 cells/ mm^2 in the controls, respectively; $P = 0.035$) and 12 weeks (group I) (0.17 ± 0.06 versus 0.0 ± 0.0 cells/mm^2 in the controls, respectively; $P = 0.014$). A similar pattern was noticed in group II at 14 weeks (0.19 ± 0.04 versus 0.0 ± 0.0 cells/ mm^2 in the controls, respectively; $P = 0.015$) (Fig. 1a). The pattern in the lung is similar to the mast cells that are adjacent to the granulomas in the liver cells of the same animals (Fig. 1b). Quantification of mast cells revealed a significant difference in the distribution in group I at 12 weeks (0.37 ± 0.10 compared to 0.0081 ± 0.008 cells/mm^2, in the controls; respectively; $P = 0.012$) and in group II at 14 weeks (0.46 ± 0.10 compared to 0.0081 ± 0.008 cells/mm^2

Table 1. Distribution of inflammatory cells in 8, 12, and 14 weeks' post-infection with *Schistosoma mansoni*.

| Immune cells | Tissue | Immune cell count | | | | Figures |
		Control	8 weeks	12 weeks	14 weeks	
Mast cells	Lung	0.0 ± 0.0	$0.054 \pm 0.02*$	$0.17 \pm 0.06*$	$0.19 \pm 0.04*$	1a
	Liver	0.0081 ± 0.008		$0.37 \pm 0.10*$	$0.46 \pm 0.10*$	1b
CD3$^+$	Lung	12.60 ± 1.36	$29.59 \pm 3.2*$	$35.0 \pm 3.92*$	$16.50 \pm 1.09*$	2a
	Liver	12.77 ± 4.01		$107.8 \pm 3.6*$	$112.6 \pm 24.75*$	2b
CD14$^+$	Lung	3.24 ± 0.85	$8.42 \pm 1.22*$	$14.99 \pm 3.17*$	$13.89 \pm 1.39*$	3a
	Liver	4.77 ± 0.40		$12.39 \pm 1.62*$	$12.75 \pm 2.17*$	3b
CD68$^+$	Lung	0.76 ± 0.46	3.48 ± 1.72	$21.70 \pm 6.6*$	$6.21 \pm 0.69*$	4a
	Liver	4.37 ± 0.47		$12.26 \pm 1.89*$	8.73 ± 1.73	4b
CD15$^+$	Lung	1.61 ± 0.44	$9.30 \pm 1.67*$	$15.95 \pm 3.90*$	$13.30 \pm 2.45*$	5a
	Liver	4.68 ± 1.08		$107.4 \pm 8.98*$	$45.01 \pm 2.80*$	5b

Data are presented as the mean ± standard error of the mean (SEM). Statistical comparisons between two groups were performed using paired and unpaired Student's t-tests with Welch correction, where appropriate, with a probability value of P < 0.05 (*) considered to be statistically significant.
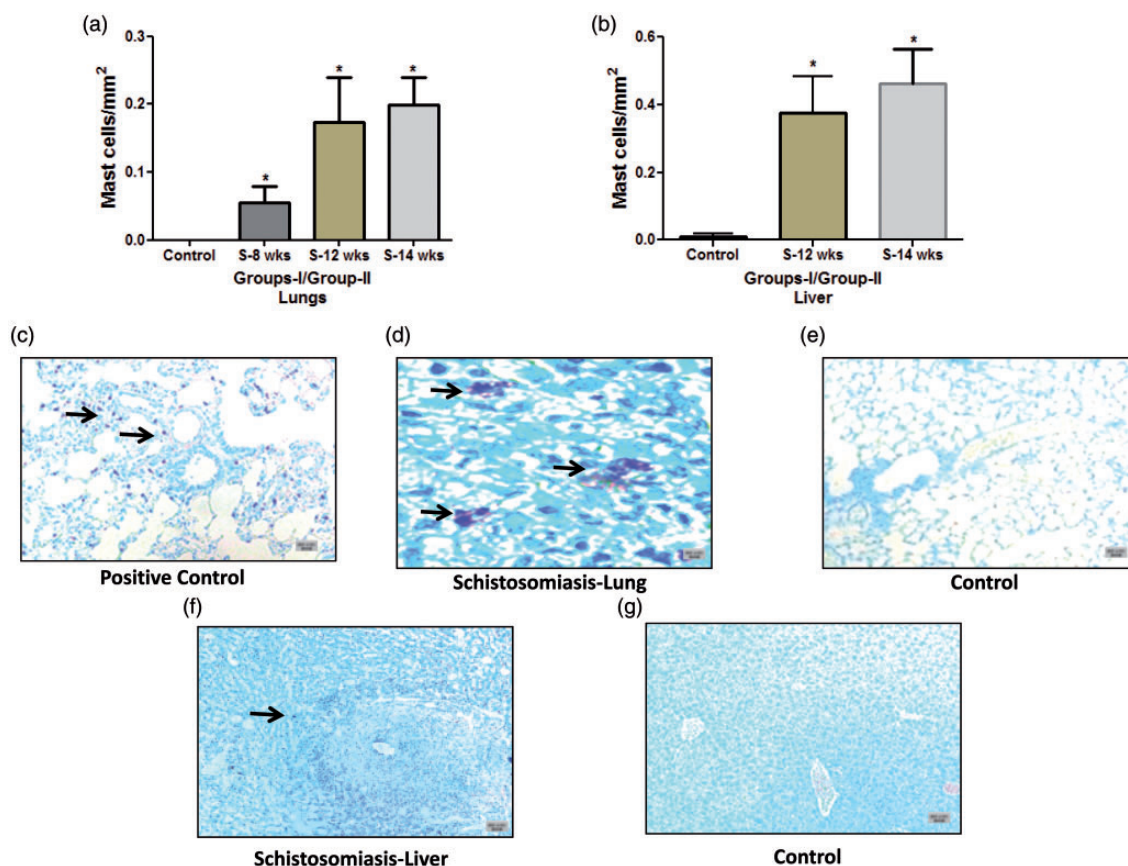
Fig. 1. Quantification and staining of mast cells in *Schistosoma*-infected and non-infected healthy controls. (a) Quantification of mast cells from control, group I (8-week and 12-week infection) and group II (14-week infection) in the lungs; and (b) from control, group I (12-week infection) and group II (14-week infection) in the liver. (c–g) Paraffin tissue sections were stained with toluidine blue to detect mast cells. Shown are representative micrographs of (c) positive control (rat lung, with induced Monocrotaline, 5×); (d) *Schistosoma*-infected lung, 40×; (e) non-infected healthy control lung, 5×; (f) *Schistosoma*-infected liver sections, 5×; and (g) non-infected healthy control liver, 5×. Arrowheads indicate the positively stained cells (purple); scale bar = 20 μm.

in the control, respectively; $P = 0.01$) (Fig. 1b). The majority of mast cells were de-granulated (increased size and less granule staining) and were mainly seen either inside or in close proximity to granuloma (Fig. 1d and 1f).

CD3$^+$ cells: The total number of CD3$^+$ cells in the lung and liver was significantly higher compared to control (Fig. 2a–i). This increase was seen at the early stage of eight weeks (29.59 ± 3.2) and at week 12 (35.0 ± 3.92) compared to the controls (12.60 ± 1.36 cells/mm^2, $P \leq 0.0001$, each) (Fig. 2a). The same pattern was noticed in group II and at 14 weeks (16.50 ± 1.09 compared to 12.60 ± 1.36 cells/mm^2 of the control, $P = 0.045$) (Fig. 2a). It was also noticed that CD3$^+$ cells were significantly increased in both groups in the liver (group 1, 12 weeks 107.8 ± 3.6 versus 12.77 ± 4.01 cells/mm^2 of the control, $P \leq 0.0001$) and in group II (112.6 ± 24.75 versus 12.77 ± 4.01 cells/mm^2 of the control, $P = 0.028$) (Fig. 2b). The acute stage granuloma was characterized by dense accretion of CD3$^+$ lymphocytes as can be witnessed from Fig. 2d and 2g.

CD14$^+$ cells: As can be seen from the respective immunostaining and quantification, the CD14$^+$ cells in the lung

and liver were significantly higher compared to the control (Fig. 3a–i). This increase was seen at the early stage of eight weeks (8.42 ± 1.22) and at week 12 (14.99 ± 3.17 compared to the controls 3.24 ± 0.85 cells/mm^2, $P = 0.001$; each) (Fig. 3a). The same pattern was noticed in group II at 14 weeks (13.89 ± 1.39 compared to 3.24 ± 0.85 cells/mm^2 of the control, $P = 0.0013$) (Fig. 3a). It was also noticed that CD14$^+$ cells were significantly increased in both groups in the liver (group 1, 12 weeks 12.39 ± 1.62 versus 4.77 ± 0.40 cells/mm^2 of the control, $P = 0.003$) and in group II (12.75 ± 2.17 versus 4.77 ± 0.40 cells/mm^2 of the control, $P = 0.036$) (Fig. 3b). The CD14$^+$ cells were excessively present in infected liver, especially inside and near the boundary of granuloma when compared to control livers (Fig. 3g and 3h).

CD68$^+$ cells: The total number of CD68$^+$ cells in the lung and liver was significantly higher compared to the control (Fig. 4a–i). This increase was seen at week 12 (21.70 ± 6.6 compared to the controls 0.76 ± 0.46 cells/mm^2, $P = 0.005$) (Fig. 4a). The same pattern was noticed in group II at 14 weeks (6.21 ± 0.69 compared to 0.76 ± 0.46 cells/mm^2 of the
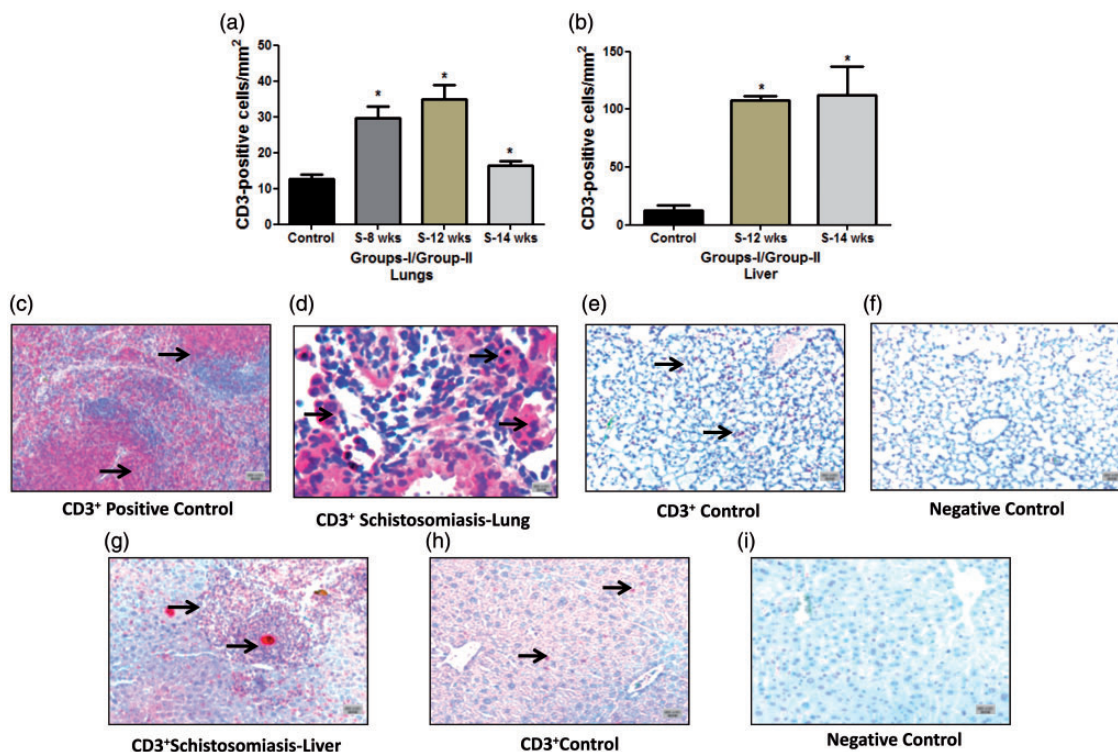
Fig. 2. Quantification and immunostaining of CD3^{+} T cells in *Schistosoma*-infected and non-infected healthy controls in groups I and II. (a) Quantification of CD3^{+} T cells from control, group I (8-week and 12-week infection) and group II (14-week infection) in the lungs; and (b) from control, group I (12-week infection) and group II (14-week infection) in the liver. (c–i) Paraffin lung tissue sections of (c) positive control mouse spleen, 5×; (d) *Schistosoma*-infected lung, 20×; (e) non-infected healthy control lung, 5×; (f) negative control lung (CD3 antibody absent), 5×; (g) *Schistosoma*-infected liver, 5×; (h) non-infected healthy control liver, 5×; and (i) negative control liver (CD3 antibody absent), 5×. The tissue section cells were stained with anti-CD3 to detect T cells. Arrowheads indicate the positively stained cells (red), scale bar = 20 μm.

controls, $P = 0.0012$) (Fig. 4a). CD68^{+} cells were also noticed to significantly increase in group I in the liver (12 weeks, 12.26 ± 1.89 versus 4.37 ± 0.47 cells/mm^2 of the controls, $P = 0.0068$) (Fig. 4b).

CD15^{+} cells: The total number of CD15^{+} cells in the lung and liver was significantly higher compared to the control (Fig. 5a–i). This increase was seen at the early stage of eight weeks (9.30 ± 1.67) and at week 12 (15.95 ± 3.90 compared to the controls 1.61 ± 0.44 cells/mm^2, $P = 0.0002$; $P = 0.0013$, respectively) (Fig. 5a). The same pattern was noticed in group II at 14 weeks (13.30 ± 2.45 compared to 1.61 ± 0.44 cells/mm^2 of the control, $P = 0.009$) (Fig. 5a). CD15^{+} cells were also noticed to significantly increase in both groups in the liver (group 1, 12 weeks 107.4 ± 8.98 versus 4.68 ± 1.08 cells/mm^2 of the control, $P \leq 0.0001$) and in group II (45.01 ± 2.80 versus 4.68 ± 1.08 cells/mm^2 of the control, $P = 0.0055$) (Fig. 5b).

Discussion

The *Schistosoma* egg antigens result in all the changes in the pulmonary vasculature by eliciting an immune response with granuloma formation. The granulomatous web recruits a variety of inflammatory cells and initiates an intricate cascade by involving inflammatory mediators such as mast cells, macrophages, dendritic cells, lymphocytes, monocytes, and neutrophils.[1–5] The understanding of inflammatory cell behavior at different stages of the immunological reaction will contribute to the understanding of the vascular pathology of schistosomiasis. The presence, involvement, and expression of each of these cells in granuloma construction are still not clear, and thus it becomes obligatory to dissect the complexity of granuloma. Based on this concept, this study identified crucial inflammatory mediators and provided some details on the role of mast cells, T cells, monocytes, macrophages, and neutrophils in schistosomiasis.

We noticed a significant progressive increase in the number of mast cells post week 8 of infection in the lung and liver when compared to uninfected healthy controls. Previous reports showed that the perivascular mast cells were increased in various pulmonary hypertension models and the majority of them were degranulated (activated) in the lungs of patients.[9,10] In these models, mast cells have a key role in the activation of matrix metalloproteinase-2 and 9,[11] which have been also recognized in the process of inflammation and tissue remodeling by Schermuly et al.[12] Thus, our findings confirm a similar increase of mast cells suggesting that these cells may contribute to pulmonary vascular remodeling.
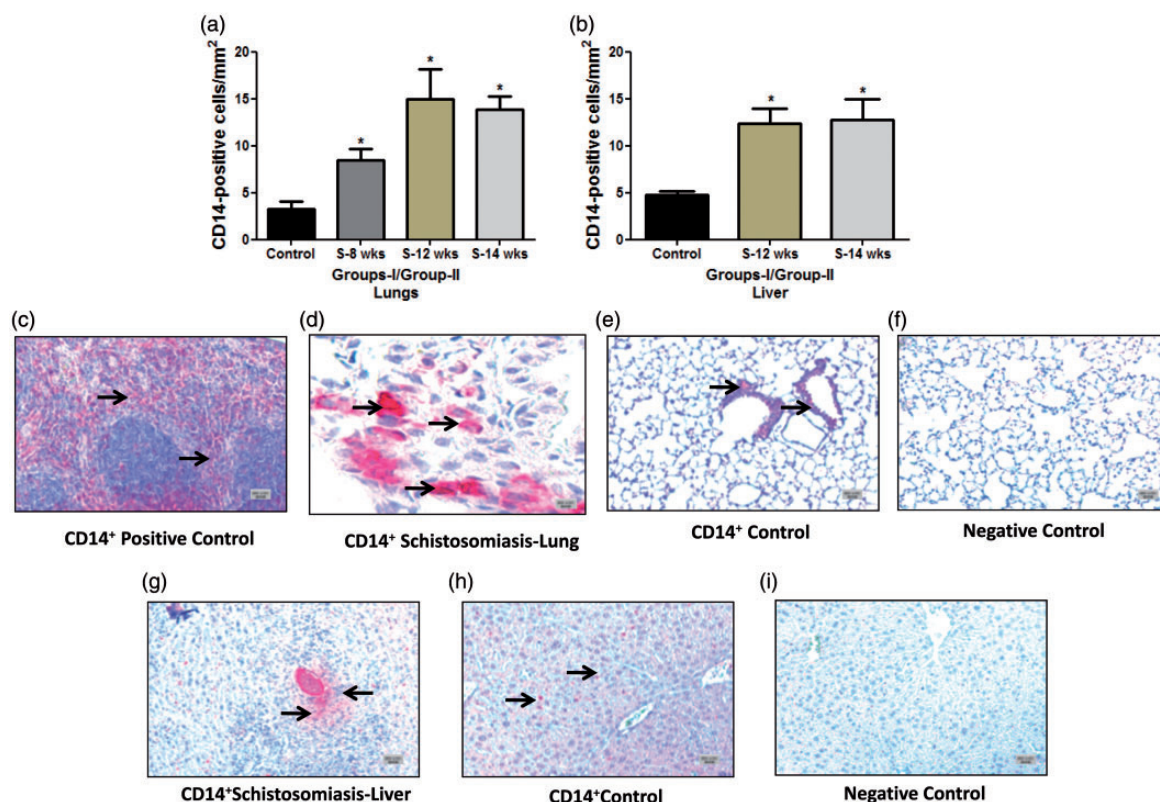
Fig. 3. Quantification and immunostaining of CD14$^+$ cells in *Schistosoma*-infected and non-infected healthy controls in groups I and II. (a) Quantification of CD14$^+$ cells from control, group I (8-week and 12-week infection) and group II (14-week infection) in the lungs; and (b) from control, group I (12-week infection) and group II (14-week infection) in the liver. (c–i) Paraffin lung tissue sections of (c) positive control mouse spleen, 5×; (d) *Schistosoma*-infected lung, 20×; (e) non-infected healthy control lung, 5×; (f) negative control lung (CD14 antibody absent), 5×; (g) *Schistosoma*-infected liver, 5×; (h) non-infected healthy control liver, 5×; and (i) negative control liver (CD14 antibody absent), 5×. The tissue section cells were stained with anti-CD14 to detect positively stained cells. Arrowheads indicate the positively stained cells (red), scale bar = 20 μm.

T cells have been implicated in several immune-pathological events during helminthic infection including schistosomiasis.[13,14] These cells may play a vital role in pulmonary vascular remodeling as they provide immunological aid for leukocytes through cytokines secretion.[15,16] The T lymphocytes undergo extensive changes in their immunological profile during the infection process from Th1, Th2, and Th17 and express a plethora of cytokines like interferon-γ, tumor necrosis factor (TNF)-α, IL-2 (Th-1 type) and later release IL-4, IL-10, and IL-13 (Th-2 type) which have been correlated well in pulmonary vascular diseases.[13,15,16] Thus, one can assume that T cells and T cell-derived cytokines can regulate the immunological response in the body and are central in the development of pathological conditions.[13,17]

In this study, we noticed a significant increase in the number of CD3$^+$ cells during the acute phase of infection in the lung and liver compared to respective controls. The recruitment and migration of CD3$^+$ lymphocytes to the granuloma peaked during 8–12 weeks and the respective immunostainings revealed CD3$^+$ cells constituted a major portion of granuloma. Furthermore, the granuloma located around eggs in the liver revealed greater expression of CD3$^+$ cells per mm^2 of area compared to those in lung. Mauad et al. also recently reported an increase in the density of CD3$^+$ T cells and mast cells in the lungs of patients that died of schistosomiasis-associated PAH.[18]

As explained above, the *Schistosoma* egg-induced granuloma is also dependent on the mobilization of macrophages and monocytes; thus, increased expression of these inflammatory cells has been reported recently.[3,7] The stimulated macrophages may present antigens to T cells leading to T cell activation and induce the release of IL-1β, IL-6, TNF-α, and IL-10, facilitating the inflammation and remodeling.[13,15,19] Tissue remodeling and fibrotic responses in chronic inflammatory conditions have been associated with activation of macrophages. The impaired production of monocyte chemoattractant protein-1, TNF-α, and interferon-γ may encourage monocyte migration into granulomas and differentiation of monocytes into macrophages, as well as macrophage activation within the granulomas.[8,13] In histological studies, the mononuclear cell inflammatory infiltrate observed around remodeled vessels, including plexiform lesions and the cells involved, are of monocytes/macrophage lineage.[19,20] Savai et al. recently reported increased perivascular monocytes (CD14$^+$) and
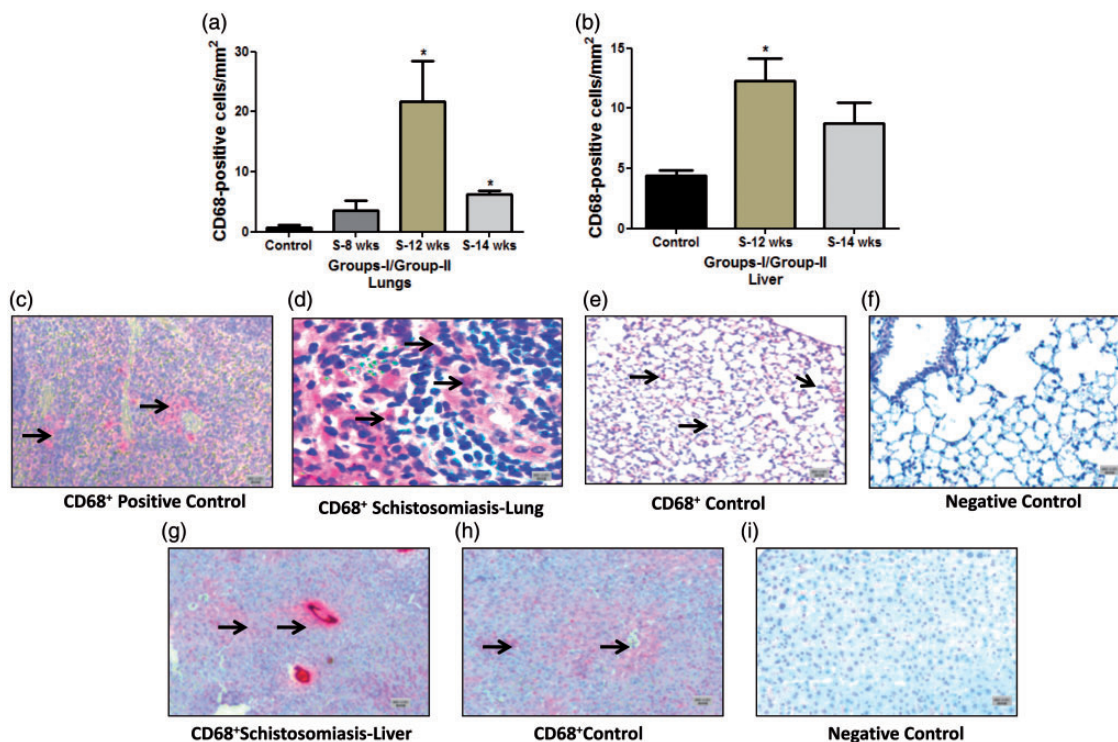
Fig. 4. Quantification and immunostaining of CD68^{+} cells in *Schistosoma*-infected and non-infected healthy controls in groups I and II. (a) Quantification of CD68^{+} cells from control, group I (8-week and 12-week infection) and group II (14-week infection) in the lungs; and (b) from control, group I (12-week infection) and group II (14-week infection) in the liver. (c–i) Paraffin lung tissue sections of (c) positive control mouse spleen, 5×; (d) *Schistosoma*-infected lung, 20×; (e) non-infected healthy control lung, 5×; (f) negative control lung (CD68 antibody absent), 5×; (g) *Schistosoma*-infected liver, 5×; (h) non-infected healthy control liver, 5×; and (i) negative control liver (CD68 antibody absent), 5×. The tissue section cells were stained with anti-CD68 to detect positively stained cells. Arrowheads indicate the positively stained cells (red), scale bar = 20 µm.

macrophages (CD68^{+}) in human idiopathic PAH.[15] In the present study, the granulomas observed in the lung and liver also consisted of monocyte and macrophage infiltration specifically at 12 weeks of infection.

Furthermore, neutrophils are generally among the first cells to be recruited to the site of inflammation, where they kill invading pathogens through phagocytosis and enzymatic digestion.[21] Precisely, they penetrate between the endothelial cells with the help of cell adhesion molecules (CAMs) and collect in the inflammatory exudates.[21] They produce a range of cytokines due to a variety of receptors on their surface such as TNF-α, IL-1, IL-8, TGF-β, and MIP. All of these modulate the immune response and leads to pulmonary vascular remodeling.[13] This may suggest that neutrophils in the granuloma can contribute to the remodeling. Our results showed a significant increase in the CD15^{+} cells after eight weeks of infection in lungs and liver. Of note, the number of CD15^{+} cells were greater in the liver than the lungs per mm[2] of area and these were more expressed inside and in close proximity to granuloma. It was recently shown that in response to the CD15 antigens, a large amount of IL-10 was secreted in vitro; IL-10 can suppress Th1 responses in animals, which may partly contribute to the Th2 dominance in early stages of

schistosomiasis. The presence of anti-CD15 antibodies in *S. haematobium* and *S. japonicum* infected individuals raises the probability for an autoimmune disorder during infections by all human *Schistosoma* species.[22]

As we learn more about the complexity of the human immune response to infection, it is becoming increasingly important to find meaningful ways of identifying and interpreting patterns of these responses. This study highlighted the importance of assaying a greater range of inflammatory cells and their contribution in S*chistosoma* infection. This integrated approach provides a powerful means of relating the immune phenotype elicited by parasite antigens and an effective means of assessing the immunological impact of experimental infection on immune-mediated disease. The above changes in the inflammatory cells and their contribution in modulating the level of inflammatory mediators confirm our original hypothesis[3,6–8] of the importance of these mediators in the remodeling process.

This paper is first to systematically characterize the quality and quantity of different inflammatory/immune cells showing dynamic changes in schistosomiasis pulmonary vascular responses. Our findings not only revealed detailed characterization of the inflammatory cells in
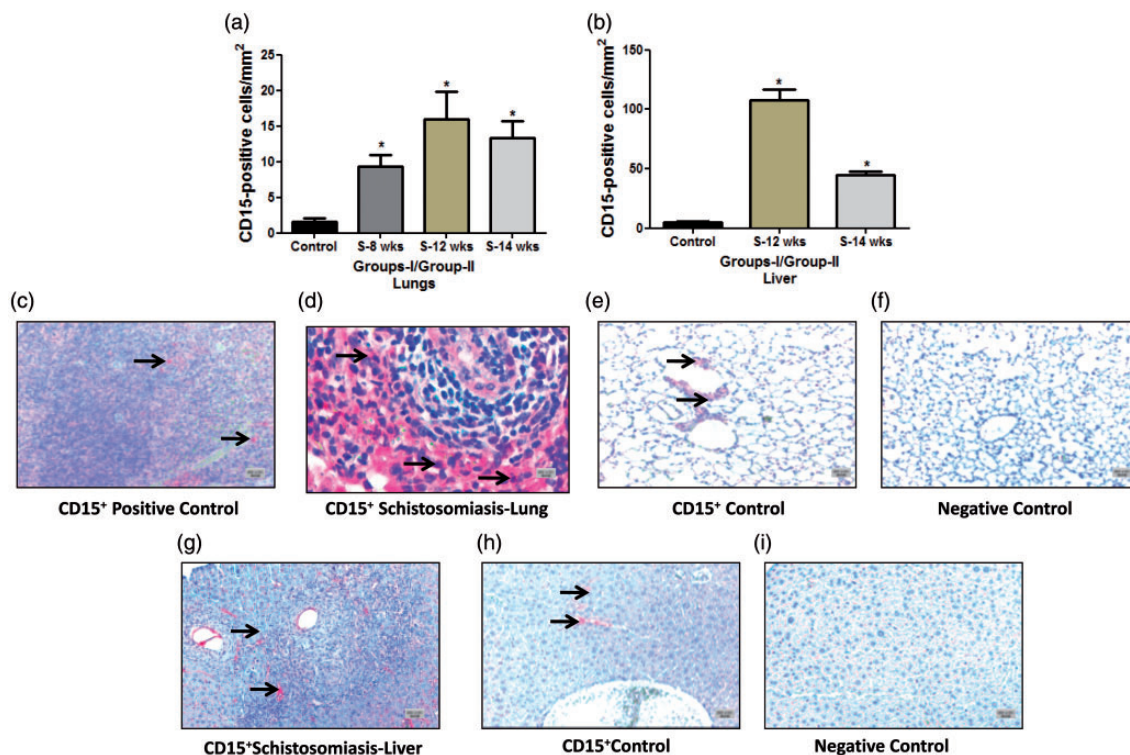
Fig. 5. Quantification and immunostaining of CD15$^+$ cells in *Schistosoma*-infected and non-infected healthy controls in groups I and II. (a) Quantification of CD15$^+$ cells from control, group I (8-week and 12-week infection) and group II (14-week infection) in the lungs; and (b) from control, group I (12-week infection) and group II (14-week infection) in the liver. (c–i) Paraffin lung tissue sections of (c) positive control mouse spleen, 5×; (d) *Schistosoma*-infected lung, 20×; (e) non-infected healthy control lung, 5×; (f) negative control lung (CD15 antibody absent), 5×; (g) *Schistosoma*-infected liver, 5×; (h) non-infected healthy control liver, 5×; and (i) negative control liver (CD15 antibody absent), 5×. The tissue sections cells were stained with anti-CD15 to detect positively stained cells. Arrowheads indicate the positively stained cells (red), scale bar = 20 μm.

schistosomiasis, but also suggest that these cells may be potential therapeutic targets for the control of inflammation.

Among the limitations, our data revealed enhanced trafficking and infiltration of several types of immune cells in the lungs and liver following infection at different doses and time points in the mouse model and not in humans. Demonstrating a similar enhancement of the inflammatory cells discussed here in lung and/or liver tissues from humans with schistosomiasis would reinforce the translational importance of the findings, which will be our subsequent study. Also, more cells such as CD4$^+$ T cells, CD8$^+$ T cells, CD209$^+$ dendrite cells, CD45$^+$ leucocytes, CCL5/RANTES$^+$, CD161$^+$ NK cells, etc., have to be mapped and more comprehensive micro-mapping of granuloma in relation to *Schistosoma* egg are important for future studies.

Acknowledgments

Conflict of interest

The author(s) declare that there is no conflict of interest.

Funding

Availability of data and materials

All tables and individual animal data will be available as a supplement online for other investigators, the link will be in the public domain upon the publication of the manuscript.

References

1. Chitsulo L, Loverde P and Engels D. Focus: Schistosomiasis. *Nat Rev Microbiol* 2004; 2: 12–13.
2. Gryseels B, Polman K, Clerinx J, et al. Human schistosomiasis. *Lancet* 2006; 368: 1106–1118.
3. Butrous G, Ghofrani HA and Grimminger F. Pulmonary vascular disease in the developing world. *Circulation* 2008; 118: 1758–1766.
4. World Health Organization. *The world health report 2002 - Reducing Risks, Promoting Healthy Life* [Internet]. Geneva: WHO. Available at: http://www.who.int/whr/2002/en/ (last accessed 6 Dec 2015).
5. Kolosionek E, King J, Rollinson D, et al. Schistosomiasis causes remodelling of pulmonary vessels in the lung in a

heterogeneous localized manner: Detailed study. *Pulm Circ* 2013; 3: 356–362.

6. Crosby A, Jones FM, Southwood M, et al. Pulmonary vascular remodelling correlates with lung eggs and cytokines in murine Schistosomiasis. *Am J Respir Crit Care Med* 2010; 181: 279–288.

7. Graham BB, Mentink-Kane MM, El-Haddad H, et al. Schistosomiasis-induced experimental pulmonary hypertension: role of interleukin-13 signaling. *Am J Pathol* 2010; 177: 1549–1561.

8. Graham BB, Bandeira AP, Morrell NW, et al. Schistosomiasis-associated pulmonary hypertension: pulmonary vascular disease: the global perspective. *Chest* 2010; 137(6 Suppl.): 20S–29S.

9. Dahal BK, Kosanovic D, Kaulen C, et al. Involvement of mast cells in monocrotaline-induced pulmonary hypertension in rats. *Respir Res* 2011; 12: 60.

10. Heath D and Yacoub M. Lung mast cells in plexogenic pulmonary arteriopathy. *J Clin Pathol* 1991; 44: 1003–1006.

11. Tchougounova E, Lundequist A, Fajardo I, et al. A key role for mast cell chymase in the activation of pro-matrix metalloprotease-9 and pro-matrix metalloprotease-2. *J Biol Chem* 2005; 280: 9291–9296.

12. Schermuly RT, Dony E, Ghofrani HA, et al. Reversal of experimental pulmonary hypertension by PDGF inhibition. *J Clin Invest* 2005; 115: 2811–2821.

13. Pearce EJ and MacDonald AS. The immunobiology of schistosomiasis. *Nat Rev Immunol* 2002; 2: 499–511.

14. Jankovic D, Cheever AW, Kullberg MC, et al. CD4+ T cell–mediated granulomatous pathology in schistosomiasis is downregulated by a B Cell–dependent mechanism requiring Fc receptor signaling. *J Exp Med* 1998; 187: 619–629.

15. Savai R, Pullamsetti SS, Kolbe J, et al. Immune and inflammatory cell involvement in the pathology of idiopathic pulmonary arterial hypertension. *Am J Respir Crit Care Med* 2012; 186: 897–908.

16. Groth A, Vrugt B, Brock M, et al. Inflammatory cytokines in pulmonary hypertension. *Respir Res* 2014; 15: 47.

17. Wynn TA, Thompson RW, Cheever AW, et al. Immunopathogenesis of schistosomiasis. *Immunol Rev* 2004; 201: 156–167.

18. Mauad T, Pozzan G, Lanças T, et al. Immunopathological aspects of schistosomiasis-associated pulmonary arterial hypertension. *J Infect* 2014; 68: 90–98.

19. Lukacs NW, Chensue SW, Smith RE, et al. Production of monocyte chemoattractant protein-1 and macrophage inflammatory protein-1 alpha by inflammatory granuloma fibroblasts. *Am J Pathol* 1994; 144: 711–718.

20. Tuder RM, Groves B, Badesch DB, et al. Exuberant endothelial cell growth and elements of inflammation are present in plexiform lesions of pulmonary hypertension. *Am J Pathol* 1994; 144: 275–285.

21. Budhiraja R, Tuder RM and Hassoun PM. Endothelial dysfunction in pulmonary hypertension. *Circulation* 2004; 109: 159–165.

22. Nyame AK, Debose-Boyd R, Long TD, et al. Expression of Lex antigen in *Schistosoma japonicum* and *S. haematobium* and immune responses to Lex in infected animals: lack of Lex expression in other trematodes and nematodes. *Glycobiology* 1998; 8: 615–624.